Synthesis and Characterisation of Ligand-bridged Tungsten and Chromium Penta- and Tetra-carbonyl Complexes

By

L. Sinuka, B.Sc. (Hons.)

Submitted to the Faculty of Science and Agriculture in partial fulfilment of the requirements for the award of the

Degree of Master of Science

in the Department of Chemistry at the University of Zululand.

Supervisor: Professor G.A. Kolawole, C. Chem., FRSC

(Dr. N Long supervised this work while at Imperial College, London)

March, 2002

DECLARATION

The work described in this dissertation was carried out in the Department of Chemistry at the University of Zululand, South Africa and at Imperial College of Medicine, Science and Technology, London, United Kingdom. All the work is my own unless otherwise stated to the contrary and has not been submitted previously for a degree at this or any other institution.

L. Sinuka

TABLE OF CONTENTS

List of Tables

List of Figures

List of Abbreviations

TBE - *trans*-1,2-(bis-4-pyridyl)ethylene

DPT - 3,6-di-2-pyridyl-1,2,4,5-tetrazine

NMR - Nuclear Magnetic Resonance Spectroscopy

MS - Mass Spectroscopy

UV-Vis - Ultraviolet-Visible Spectroscopy

IR - Infrared Spectroscopy

TLC - Thin Layer Chromatography

MLCT - Metal-to-ligand charge-transfer

CT - Charge transfer

LF - Ligand field

IL - Intra ligand

HOMO - Highest occupied molecular orbital

LUMO - Lowest unoccupied molecular orbital

THF - tetrahydrofuran

bpy - 2,2′-bipyridine

bpym - 2,2′-bipyrimidine

bppz - bipyridylpyrazine

bptz - 3,6-di-2-pyridyl-1,2,4,5-tetrazine

abpy - amino-2,2′-bipyridine

Acknowledgements

I am indebted to:

Professor G.A. Kolawole (University of Zululand, South Africa) and Dr. N. Long (Imperial College of Medicine and Technology, London, United Kingdom), for the opportunity to carry out research in the UK and for helpful discussions and constructive criticisms.

Professor P. O'Brien for financial assistance especially during my stay in London.

The Chemistry Department academic and technical staff at the University of Zululand, and the technical staff at Imperial College for the help offered.

My friends and colleagues at the University of Zululand for their continued interest in my work.

My family for their love and support.

The National Research Foundation (NRF), South Africa, and the Royal Society, United Kingdom, for financial assistance.

ABSTRACT

Ligand bridged metal carbonyl complexes of the form $[_5(CO)MLM(CO)_5]$, $[_4(CO)MLM(CO)_4]$ and $[_4(CO)ML]$, where M is either tungsten or chromium and L is either trans-1,2-(bis-4-pyridyl)ethylene(TBE) or 3,6-di-2-pyridyl-1,2,4,5-tetrazine (DPT) have been synthesised. They were characterised using IR, UV-Vis and NMR, MS, TLC and microanalysis. Electronic spectral studies showed that both the dinuclear, $[_4(CO)CrDPTCr(CO)_4]$ and mononuclear, $[_4(CO)CrDPT]$ complexes have MLCT transitions at 900.88 nm and 652.52 nm respectively. The dinuclear MLCT is more intense and broad and is deemed to have overlapped with the d-d transitions observed in the mononuclear complex at 909.45 nm. However, intra-ligand transitions were observed at 279.97 nm, 303.53 nm and 382.75 nm for both mononuclear and dinuclear complexes. Photoluminescence spectra showed two emissions for $[TBE\{W(CO)_5\}_2]$; with the emission at 530 nm originating from an MLCT transition, and the one at 353 nm originating from an intra-ligand transition. For $[_4(CO)CrDPTCr(CO)_4]$ and $[_4(CO)CrDPT]$, a single broad emission was observed at 523 nm and 460 nm respectively. A small peak at 400 nm in the dinuclear complex is observed and is tentatively attributed to an intra-ligand transition. A structure of distorted octahedron is proposed for pentacarbonyl*trans*-1,2-(bis-4-pyridyl)ethylenetungsten.

CHAPTER 1

INTRODUCTION

1.1. Historical Background

Ligand bridged metal carbonyl complexes have been the subject of intensive research ever since the Creutz-Taube complex was made[1,2]. It was shown that these complexes would have different properties depending on the metal and/or ligand involved. This served as a basis for research; looking for metal/ligand combinations that will enhance a certain property of the complex (e.g. intra-molecular electron-transfer). Factors being investigated are stability, electron transfer, photochemistry, ligand effects, and solvent effects on these properties. The complexes generally are singly or doubly substituted metal carbonyls, with the substituent being the chosen ligand.

For metal hexacarbonyls, they have the following general structure $[_5(CO)MLM^*(CO)_5]$ and $[_4(CO)MLM^*(CO)_4]$, where M/M* is the metal/metals used, and L is the bridging ligand. For chelating ligands, where the coordinating atoms are close to each other, the latter complex is usually found. Complexes with one metal centre, which could be of the form $[_5(CO)ML]$, $[_4(CO)ML_2]$, and $[L^*M(CO)_4]$ (L* is a chelating ligand) have also been made[3]. The electrochemical and photo-physical properties have and are being investigated. Various metals and ligands have been used to make these complexes[3,4]. The various complexes produced have obviously different properties, e.g. charge-transfer may occur at a shorter wavelength for one, but at a longer wavelength for the other. Electronic studies carried out show that metal-to-ligand charge-transfer transition is ligand

sensitive and occurs in the region 400 nm to 900 nm. Also the effect of the length of the bridging ligand, as well as the extent of its conjugation, have been studied[5-9]. Adding a second metal centre to a mononuclear complex alters the properties of that complex considerably, e.g. the metal-to-ligand charge-transfer transition is red shifted in some complexes[10]. In addition to MLCT, there are two other transitions, ligand field/ d-d transition and intra-ligand transitions; the former occurs at an energy that is lower than the MLCT whilst the latter occurs at a higher energy than the MLCT.

Photo-physical studies indicate that some of the complexes do emit radiation after absorbing an incident radiation, albeit the emitted radiation is of a longer wavelength than the one absorbed[11,12]. Photoluminescence studies of complexes of the type $[_5(OC)WLW(CO)_5]$ show a broad, single emission band at low energies[13,14]. This emission occurs in complexes that have low-lying ligand π^* orbitals, and is evidence of the MLCT character of the emission. The fact that complexes whose ligand field transitions are lower in energy than their MLCT transitions are not emissive is further proof of this assignment[14]. In most studies the excitation wavelength is in the region longer than 300 nm. $[M(CO)_4L]$ or *cis*-$[M(CO)_4L_2]$ exhibit a dual emission, the low energy emission is thought to be of MLCT in character as it lies too low in energy to arise from a ligand field transition. The higher energy emission is of the MLCT excited state, because it exhibits solvent shift similar to those of the MLCT band absorption[15].

Electrochemical investigations have yielded results that show redox behaviour in the complexes[16]. The binuclear complexes are more easily reduced than their mononuclear counterparts, and the ligand is the least readily reduced[13]. This is due to the stabilisation (lowering) of the π^* orbital of the ligand in the binuclear complexes. A series of Ru(II) – Ru(III) dimer were shown to undergo two one electron oxidation; where the ligands were pyrazine, pyrimidine and 4,4-bipyridine[17]. This results in a phenomenon called intramolecular charge-transfer which occurs across the ligand bridge; modification of both the metal centre and the ligand has resulted in the optimization of this process[10]. The interest in this type of complex is largely due to these properties, which could have some possible industrial or technological applications, e.g. solar cells, conductors and sensitisers[18].

1.2. Metal Carbonyls

The metal carbonyls are complexes on their own, and have been extensively studied. Their structure and bonding have been studied; carbonyls bond either as terminal or bridged substituents. (Fig. 1.1.).

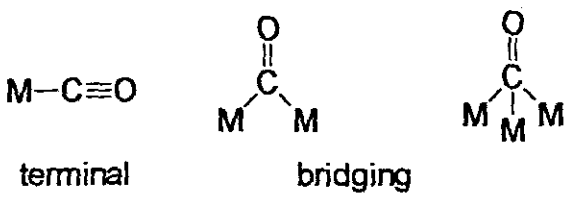

Fig. 1.1. Carbonyl bonding modes

The metal-to-carbon bond is not an ordinary single/ double bond, but an intermediate between a single and a double. Therefore it is much shorter and stronger than the corresponding single bond, but longer and weaker than the corresponding double bond. So their structure is a resonance hybrid of the following structure,

$$M{-}C{\equiv}O \longleftrightarrow M{=}C{=}O$$

The reason for this is the π^* acceptor ability of the carbonyl ligand. The bond occurs by the donation of two electrons by the carbonyl, and is followed by the $d\pi(M)$ to the $\pi^*(CO)$ back bonding especially with low valent metals[19]. This will happen if the π^* orbital of the carbonyl is directly aligned with the $d\pi$ orbital of the metal to ensure maximum overlap. (Fig. 1.2.).

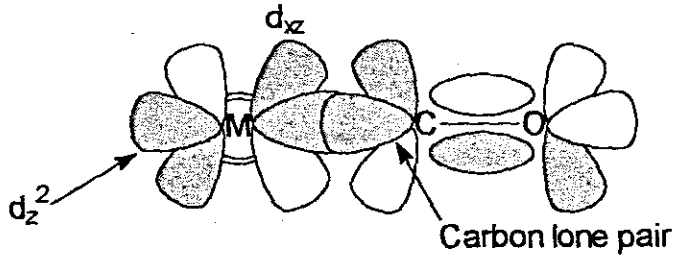

Fig. 1.2. Bonding interactions of CO with transition metals.

The extent of backbonding is highly dependent on the charge on the metal, and

on the ligand employed. For example, in the following complexes, the ν(CO) varies with charge as follows; $[Fe(CO)_4]^{2-}$ (1790 cm^{-1}) < $[Co(CO)_4]^-$ (1890 cm^{-1}) < $[Ni(CO)_4]$ (2060 cm^{-1}).

This reflects the decreasing extent of back bonding as the metal oxidation number becomes less negative[20].

1.2.1. Electronic Structure

The carbonyl complexes exhibit three transitions, viz. ligand field (LF), intraligand (IL) and charge transfer (CT) transitions. A charge transfer transition can be metal to ligand charge transfer (MLCT) or ligand to metal charge transfer (LMCT). Upon complexation with the ligand (L), the orbital structure changes with the changes in the energies of the orbitals. (Fig. 1.3.).

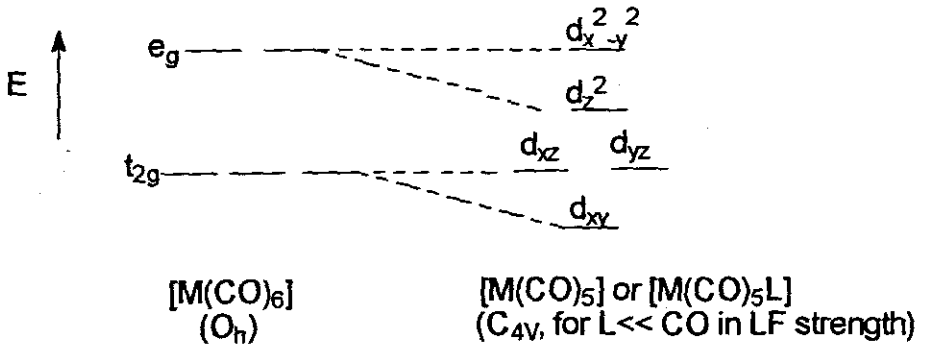

Fig. 1.3. One electron level diagram for O_h and C_{4v} complexes

For C_{2v} (Fig. 1.4), the LF transitions must be lower in energy since the two unoccupied higher orbitals (dz^2 and dx^2-dy^2) are the lowest as compared to the

other symmetries. The CT energy position is dependent on both the length and conjugation of the ligand, and the metal.[21]

In complexes where L has no low lying π* orbitals, the lowest absorption system has been associated with the $e^4b_2^2 \rightarrow e^3b_2^2a_1^1$ transition[22]. This is because the difference in energy is very much bigger between the π* orbital of the carbonyl and the t_{2g} orbital which house the electrons, than it is between e_g and the same t_{2g} metal orbitals (Fig. 1.4.).

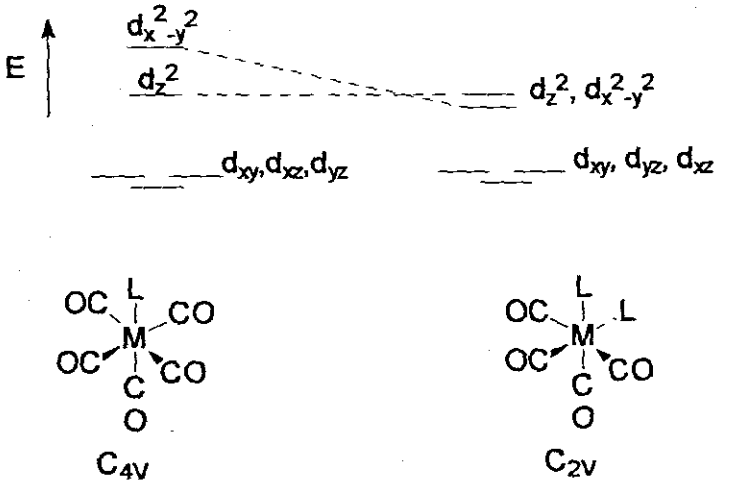

Fig. 1.4. One electron diagrams for C_{4v} and C_{2v} complexes

If L has low-lying π* orbitals, MLCT may be the lowest energy transition in the $[_5(CO)ML]$ (C_{4v}) complexes. The MLCT is also affected by the substituents on the ligand; electron-releasing substituents result in a higher energy MLCT, and vice versa. It is also solvent sensitive in that more polar or polarisable solvents give blue-shifted maxima. Therefore it is possible to resolve overlapping LF and MLCT bands by varying the solvents. Also complexed ligands with low-lying

excited states often exhibit IL transitions; these are similar to those found in the free ligand. Complexes of C_{2v} symmetry have also been studied, and the *cis*-$[M(CO)_4L_2]$ or $[_4(CO)ML^*]$ (L^* is a bidentate ligand) have similar transitions as the $[_5(CO)ML]$ species differing in energy positions.[23]

1.2.2. Photo-reactions

Carbonyl complexes of Cr, Mo and W have extensive photochemistry. Though substitution is the most dominant reaction, examples of isomerisation, linkage isomerisation, and intra-ligand isomerisation are known.

1.2.3. Photo-susbtitution

Chemistry involving ligand exchange and substitution dominates the excited states processes of $[M(CO)_6]$ complexes. The following steps were postulated for this process,

$$M(CO)_6 \xrightarrow{h\nu} M(CO)_5 + CO \qquad (A)$$

$$M(CO)_5 + CO \xrightarrow{k} M(CO)_6 \qquad (B)$$

$$M(CO)_5 + L \xrightarrow{k^*} M(CO)_5L \qquad (C)$$

The $[M(CO)_5]$ species has a C_{4v} symmetry and is scavengeable by virtually any nucleophile. Photolysis of the $[M(CO)_5L]$ leads to two possibilities, and that is the loss of another CO molecule (D) or the loss of the ligand, L (E)[24-26].

$$M(CO)_5L \xrightarrow{h\nu} M(CO)_4L + CO \qquad (D)$$

$$M(CO)_5L \xrightarrow{h\nu} M(CO)_5 + L \qquad (E)$$

The efficiencies of the above processes depend on the nature of the ligand, for example, when L is THF process (D) is fairly significant. Also these processes are sensitive to the wavelength of the lamp.

1.3. The ligands

Ligand selection is very important since the properties of the ligand will, in addition to other factors, invariably determine the nature and stability of the complexes. Like the carbonyls, some heterocycles are electron acceptors to varying extents, and ligands with electron donating substituents are generally strong electron donors, the opposite is true for those with electron withdrawing substituents[27].

Ligands that are strong π-acceptors of back-bonded electrons have a tendency to weaken the metal-to-carbon bond of the terminal carbonyl *trans* to it, resulting in the ease of the second substitution. Some examples are:
$[(PF_3)_3Mo(CO)_3]$, 2055 cm^{-1}, 2090 cm^{-1}; $[(PPh_3)_3Mo(CO)_3]$, 1835 cm^{-1},1934 cm^{-1}; $[(py)_3Mo(CO)_3]$, 1746 cm^{-1}, 1888 cm^{-1}[128].

Steric effects are also very important, for instance for a bidentate ligand (e.g. DPT) the bite angle will determine the stability of the complex. A natural bite angle is defined as the preferred chelation angle determined by its backbone[29].

Ligands to be used in this work are 1,2-[bis(4-pyridyl)]ethylene and 3,6-(di-2-pyridyl)-1,2,4,5-tetrazine (Fig 1.5.)

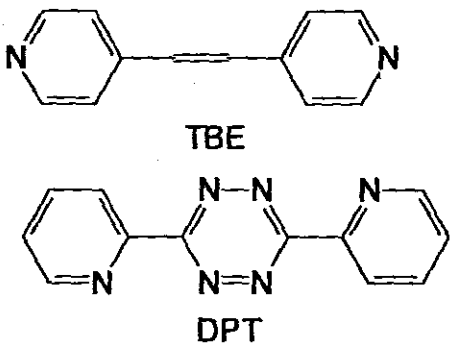

Fig. 1.5. Structures of the ligands used.

As can be seen from above, TBE is just two pyridine moieties bound together by the ethylene group at carbon-4. The presence of the electron rich ethylene group increases the electron density of the compound resulting in increased tendency for nucleophilic mode of attack. It also makes the ligand to have extended conjugation. DPT is also simply two pyridines bound through carbon-2 to 1,2,4,5-tetrazine via carbon-3 and carbon-6, and it is more conjugated than TBE. Therefore their chemistry is similar to that of pyridine[30].

1.4 Instrumental analysis

1.4.1 Infrared spectroscopy

Infrared spectroscopy has been a valuable tool in studies concerning transition metal carbonyl complexes. It has been used to monitor the reaction progress, by taking successive spectra as the reaction goes on, and when the hexacarbonyl absorption band completely disappears the reaction has run to completion. The carbonyl absorption splitting tells us about the extent of substitution of the carbonyls in the original starting hexacarbonyl.

From symmetry considerations, three vibrational modes are expected for a symmetric octahedral metal hexacarbonyl, $[M(CO)_6]$, complex, which is our starting material. The modes are shown in Fig. 1.6.

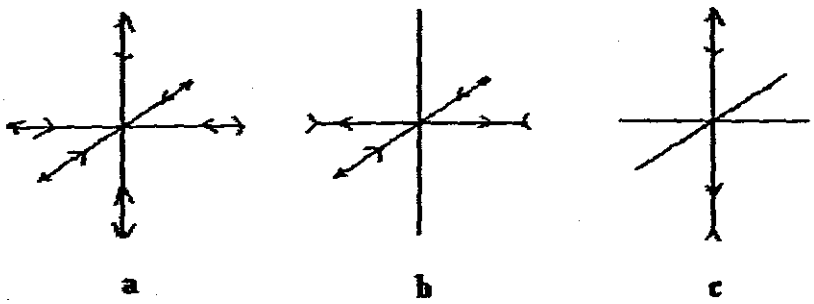

Fig. 1.6. Metal hexacarbonyl vibrational modes.

where a represents A_{1g}, b represents E_g, and c representing T_{1u} vibrational modes.

Only the last one is infra-red active, and the two Raman active, so only a single infra-red band is observed for a symmetrical metal hexacarbonyl.

For the C_{4v} singly substituted $[LM(CO)_5]$ complex, three bands are expected, and that comes from two A_1 and E vibrational modes, shown in Fig. 1.7.

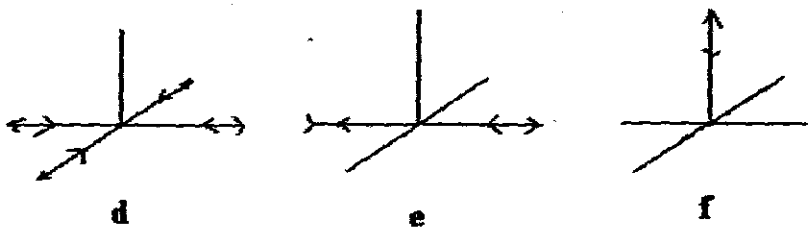

Fig. 1.7. Pentacarbonyl vibrational modes

d stands for the A_1^{1b} vibrational mode, e for E vibrational mode, and f for the A_1^{1a} vibrational mode; the E vibrational mode, which is doubly degenerate, corresponds to the infra-red allowed T_{1u} (triply degenerate) vibrational mode, and will be the dominant band of the three. This band will be positioned between the two A_1 bands, with the weaker A_1^{1b} band at a higher frequency than the E band, and the other A_1^{1a} at the lowest frequency.

For [cis-$L_2M(CO)_4$] complex, which has a C_{2v} symmetry, the expected number of bands is four, arising out of the vibrational modes shown in Fig. 1.8.

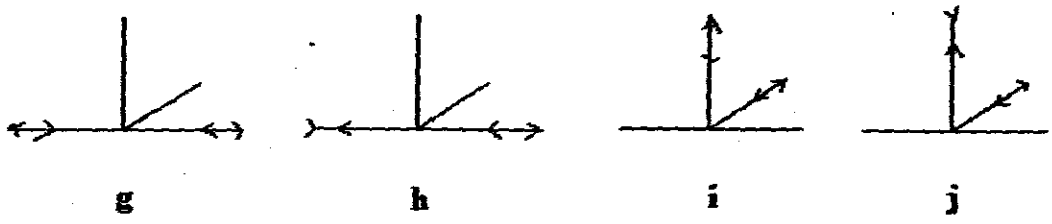

Fig. 1.8. Tetracarbonyl vibrational modes

where g stands for the A_1^{1a}, h for the B_1, i for the A_1^{1b}, and j for the B_2 vibrational modes. B_1, which corresponds to the hexacarbonyl T_{1u} vibrational mode, will have the strongest intensity and the A_1^{1a}, which is almost forbidden, will have the weakest intensity. The other two, which are slightly similar, will have comparable intensities.

Another way of looking at infrared spectra of metal hexacarbonyls is applying group theory and symmetry to matrix representations as outlined below:

Judging from the structure of the ligands involved and similar complexes previously reported, the possible molecular structures of the complexes are given in Figure 1.9.

The ligand for the complex on the top is TBE and the ligand for the one on the bottom is DPT. Mononuclear derivatives have also been made. One of the carbonyls has been knocked off the TBE complex, leaving a pentacarbonyl moiety. This has reduced the symmetry of the metal hexacarbonyl starting material from octahedral (O_h) to C_{4v}, and to C_{2v} for tetracarbonyl DPT complex.

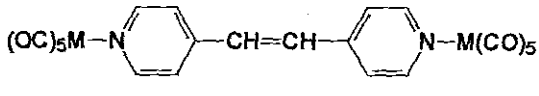

TBE Complex

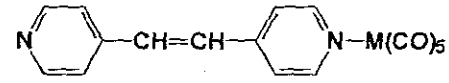

TBE Complex

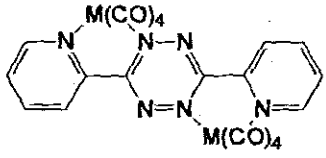

DPT Complex

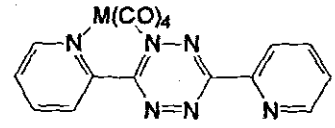

DPT Complex

Fig. 1.9. Possible structures of the complexes

These symmetries have character tables shown in Tables 1.1 and 1.2 respectively. From the character tables we can determine which of the vibrational modes are actually allowed and how many times they occur from the irreducible representation using the equation 1,

$$a_p = 1/g \sum_{R's} n_R \chi R \chi_p R \qquad (1)$$

where: a_p represents the number of times that the irreducible representation p occurs in any representation,

g the number of symmetry operations in that group,

$\sum_{R's}$ the summation over all classes,

n_R the number of operations in a class,

χR the character in the reducible representation,

$\chi_p R$ the character in the irreducible representation, p, for any operation R.

Table 1.1: C_{4v} character table

C_{4v}	E	$2C_4$	C_2	$2\sigma_v$	$2\sigma_d$		
A_1	1	1	1	1	1	T_z	x^2+y^2, z^2
A_2	1	1	1	-1	-1	R_z	
B_1	1	-1	1	1	-1		x^2-y^2
B_2	1	-1	1	-1	1		xy
E	2	0	-2	0	0	$(T_x, T_y), (R_x, R_y)$	(yz, zx)

Table 1.2: C_{2v} character table.

C_{2v}	E	C_2	σ_v	σ_v'		
A_1	1	1	1	1	T_z	x_2, y_2, z_2
A_2	1	1	-1	-1	R_z	xy
B_1	1	-1	1	-1	T_x, R_y	zx
B_2	1	-1	-1	1	T_y, R_x	yz

To apply this practically to the C_{2v} symmetry of the complex shown in Fig. 1.10 we have to consider the matrix representation for each of the operations of the point group. These are C_2, E, σ_v and σ_v'. The complex shown in Fig. 1.10 is a *cis* C_{2v} complex.

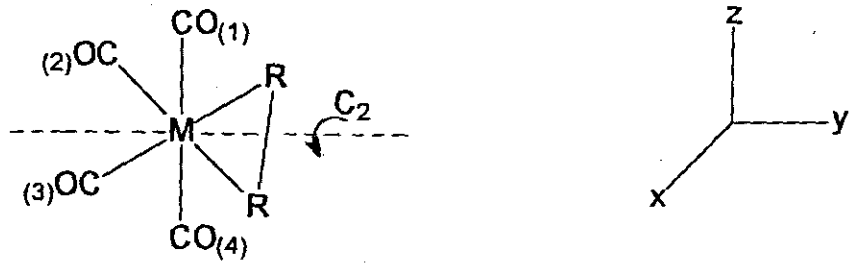

Fig. 1.10. A *cis*-$[M(CO)_4L]$ complex; C_{2v} point group

We can consider C_2 to be on the y-axis, σ_v on the xy-plane and σ_v' on the yz-plane. If we consider only the four stretching vibrations (instead of 3N-6) as our point of interest, we can create matrices for each operation, and the character of these are:

$$\chi(E) = 4,\ \chi(C2) = 0,\ \chi(\sigma v) = 2, \text{ and } \chi(\sigma v') = 2.$$

Therefore, $\Gamma_{red} = 4 + 0 + 2 + 2$

To find the irreducible representation we will use eq. 1 and the character table shown in Table 1.1 above.

Then, $a_{A1} = \frac{1}{4}[(1 \times 4 \times 1) + (1 \times 0 \times 1) + (1 \times 2 \times 1) + (1 \times 2 \times 1)]$

$= \frac{1}{4}[4 + 0 + 2 + 2] = 2$

$a_{A2} = \frac{1}{4}[(1 \times 4 \times 1) + (1 \times 0 \times 1) + (1 \times 2 \times -1) + (1 \times 2 \times -1)]$

$= \frac{1}{4}[4 + 0 - 2 - 2] = 0$

$a_{B1} = \frac{1}{4}[(1 \times 4 \times 1) + (1 \times 0 \times -1) + (1 \times 2 \times 1) + (1 \times 2 \times -1)]$

$= \frac{1}{4}[4 + 0 + 2 - 2] = 1$

$$a_{B2} = \frac{1}{4}[(1 \times 4 \times 1) + (1 \times 0 \times -1) + (1 \times 2 \times -1) + (1 \times 2 \times 1)]$$

$$= \frac{1}{4}[4 + 0 - 2 + 2] = 1$$

Therefore $\Gamma_{irred} = 2A_1 + B_1 + B_2$

So for C_{2v} we have four modes of CO stretching vibrations and all these are infra-red active.[19] The number of bands may be smaller since the transitions could be of low intensity or degenerate with other allowed transitions. Using literature and experience these modes can be assigned to certain frequencies. For example for [M(CO)$_4$bpy] these are $A_1^{1a} = 2000$ cm^{-1}, $B_1 = 1866$ cm^{-1}, $A_1^{1b} = 1847$ cm^{-1} and $B_2 = 1813$ cm^{-1} [10].

Coming to the C_{4v} point group, a similar approach will be used for the five stretching vibrations. The operations of this point group are E, C_4^1, C_4^3, C_2, σ_v, σ_v', σ_d, and σ_d'. Applying these to the pentacarbonyl moiety shown below (Fig. 1.11).

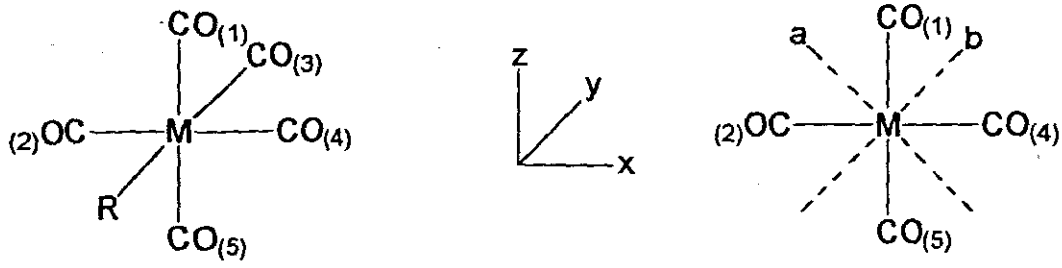

Fig. 1.11: Pentacarbonyl complex, [M(CO)$_5$L]; C_{4v} point group

σ_v and σ_v' are actually on the xy and the yz planes respectively, and the two σ_d's are on the plane bisecting the right angled OC - M – CO bonds on both sides of the metal centre along the R – M – CO bond, which is perpendicular to the plane of the paper (right hand side of Fig. 1.12).

$$\Gamma_{red} = \chi(E) + \chi(C^1_4) + \chi(C^3_4) + \chi(C_2) + \chi(\sigma v) + \chi(\sigma v') + \chi(\sigma d) + \chi(\sigma v')$$

$$= 5 + 1 + 1 + 1 + 3 + 3 + 1 + 1$$

To find the irreducible representations we use eq. 1 and the C_{4v} character table shown in Table 1.2.

Therefore:

$$a_{A1} = 1/8\,[(1\times 5\times 1) + (2\times 1\times 1) + (1\times 1\times 1) + (2\times 3\times 1) + (2\times 1\times 1)]$$

$$= 1/8[\,5 + 2 + 1 + 6 + 2] = 2$$

Similarly, $a_{A2} = 1/8[\,5 + 2 + 1 - 6 - 2] = 0$,

$$a_{B1} = 1/8[\,5 - 2 + 1 + 6 - 2] = 1,$$

$$a_{B2} = 1/8[\,5 - 2 + 1 - 6 + 2] = 0,$$

and $a_E = 1/8[\,10 + 0 - 2 + 0 + 0] = 1$

Therefore, $\Gamma_{irred.} = 2A_1 + B_1 + E$

Again literature confirms this result and for some complexes, frequencies have been assigned to these representations (or vibrational modes)[9].

1.4.2 UV-visible Spectroscopy

UV-Vis spectroscopy has been used extensively in gaining understanding of the electronic properties of these complexes. As mentioned in the introduction, there are mainly three processes associated with the absorption of UV-Vis radiation, viz. the intra-ligand $\pi \rightarrow \pi^*$ or $n \rightarrow \pi^*$ transition, the charge transfer transition, and the ligand field d-d transitions. The energy of the charge-transfer transition can provide information about the electronic structure of the complexes; a low energy CT suggests a low lying π^* lowest occupied molecular orbital (LUMO) characteristic of the ligand. Metal oxidation states also affect the CT.

Previous studies on other α-diimine (DPT/bptz) tetracarbonyl complexes have shown that the MLCT band can comprise of several transitions from filled d levels to the lowest unoccupied π^* orbital of the ligand. The dominating, symmetry allowed component is a $\pi^* \leftarrow d_{yz}$ transition[31]. The long wavelength absorption maxima, which, for the ligands, are already in the visible region due to $n \rightarrow \pi^*$ transitions and lie between 550 nm and 700 nm for the mononuclear complexes, reach the near infrared region in the binuclear complexes.[10]

1.4.3 Nuclear magnetic resonance spectroscopy.

NMR is a valuable tool used in characterising the product. Both ^{1}H and ^{13}C NMR have been used in characterising molecules and complexes, one complements the other. Variations in the technique have been developed with the intention of

maximising its usefulness, e.g. Nuclear Overhauser Effect Spectroscopy (NOESY) and others. To characterise these complexes, a NMR spectrum of the free ligand is taken and compared to the spectrum of the product formed; this will provide information as to whether a dimer or a monomer has been formed. For instance, in a binuclear symmetric product the spectrum of that product is similar to that of the free ligand, but just de-shielded, an example is trans-1,2-(bis-pyridyl)ethylene complexes.

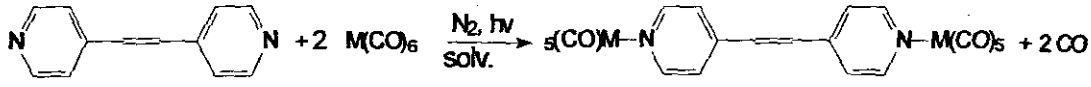

In the above reaction, the symmetry of the ligand has been preserved, but due to electron donation by the nitrogen atoms when coordinating to the metals, the proton/ carbonyl signals will be deshielded. If only one of the nitrogen atoms is bonded, then the NMR spectrum of the mononuclear complex will reflect that by unsymmetrical splitting of the original free ligand signals. The ligand atom will have different electronic environments resulting in a different, probably more complex product spectrum.

1.4.4 Mass spectrometry

This technique is also used for product characterisation. In mass spectroscopy the complex is bombarded by an electron beam; these will knock off an electron from the complex. This generates a molecular ion, which starts a process of fragmentation of the molecule. The mass of the molecular ion should be the highest in the mass spectrum, and should correspond to the molecular mass of the complex. The fragment should also correspond with the mass of the expected fragment based on established fragmentation patterns. The main feature for the mass spectra of these complexes is that they show a couple of significant peaks. One is due to the loss of the HCN group from the ligand and the other to the successive loss of the carbonyl groups. Carbocations formed from the ligands are stabilised by electron relocation through mesomeric effects, in addition to the inductive effects.

1.4.5. Cyclic voltammetry

Cyclic voltammetry is one of the variations of the potential sweep experiments. Here, the analyte is dissolved in a non-volatile solvent, and an electrolyte is also added to the solution for efficient charge movement. Three electrodes are inserted, known as the working, reference and the auxiliary electrodes, and current is applied to the working electrode with stirring to enhance charge migration. A potential sweep starting from a positive to a negative potential is

applied, and the direction is reversed at the end, i.e.switching potential. This generates current, which is cathodic first and then anodic after the potential switch; the analyte is reduced in the forward sweep and re-oxidised upon switching of the potential. If the current *vs* the potential is plotted, a cyclic voltammogram is produced, and from it one can tell whether a redox process has indeed taken place, whether it is reversible or not, and how many electron are involved. For a fully reversible process, the cathodic and the anodic current graphs are similar to each other even though the anodic curent graph is usually inverted, and they are dissimilar for irreversible processes.

Also, if the difference between the cathodic and the anodic peaks is 59 mV or a multiple of it, then one or more electrons is involved.

In mononuclear complexes the position of the formally metal reduction is quite strongly dependent on the degree of unsaturation of the pyridyl ligands, whereas the reduction potential are essentially constant. This suggest that the redox orbitals involved in the reductions have considerable ligand based character whereas the oxidation are strongly metal centred.[32,33]. Brewer, *et al.* observed that monometallic complexes display one reversible oxidation corresponding to the Fe(III)/(II) couple, while two reversible oxidations, separated by 140-150 mV, are observed for the bimetallic complexes[34]. In the case of reductive processes, the pyridyl ligands (bpym, bppz, bptz, abpy) already exhibit reversible first and irreversible second reduction waves in their cyclic voltammograms[35].

1.5.5. Photoluminescence

Emission spectroscopy is one of the properties to be investigated for the compounds we are dealing with. We expect that these complexes will fluoresce since the ligands are highly conjugated; this is because the $\pi^* \leftarrow \pi$ transition which is fluorescent is of lower energy that the non-fluorescent $\pi^* \leftarrow$ n transition for the ligands. This means that the distance between π orbital and the π^* orbital of the ligand is shorter than the one between the n and π^* orbitals. Conjugation and structural rigidity results in the compound's ability to fluoresce, e.g. fluorescein. Another phenomenon which is observed is phosphorescence; this is similar to fluorescence but results from intersystem crossing in the molecule before it returns to the ground state. Phosphorescence occurs at longer wavelength than fluorescence, and also the excited electron is in the triplet state rather than the singlet state of fluorescence. Other process that compete with fluorescence are vibrational relaxation and external quenching. Internal conversion precedes vibrational relaxation, and external quenching is preceded by intersystem crossing. These are all represented in Fig. 1.12.

The straight arrows represent radiative processes and the wavy ones the non-radiative. In the middle of the diagram there are arrows pointing up and down, these represent excitation (photon absorption) and fluorescence, respectively. On the left, the wavy arrows represent non-radiative relaxation, and on the right we have external quenching (wavy) and phosphorescence (straight). *a* represents internal conversion, *b* intersystem crossing and *c* is vibrational relaxation (wavy).

Fig. 1.12. Molecular excitation routes for subsequent deactivation and phosphorescence.

Also emission resulting from MLCT has been reported for our types of complexes, with dual emission observed for $[M(CO)_4L]$ type complexes [8,10]. Fluorescence usually occurs at longer wavelengths than absorption (excitation). This is due to the fact that before fluorescence actually occurs, vibrational relaxation reduces the energy (and therefore increases the wavelength of the system). Here the excited electron looses energy until it reaches the lowest level of that excited electronic level (see c in Fig. 1.12.).

Only a few metal carbonyls luminesce. Wrighton, *et al.* [14] observed luminescence in a C_{4v} complex of the general formula $[_5(CO)W\text{-}N$ electron donor]. This emission was attributed to a LF triplet-to-singlet transition. The emission lifetimes

are in the order 10^{-6} to 10^{-5} s range, typical of heavy metal complexes. Pyridine-based complexes with the lowest MLCT excited states have emissions whose lifetimes are longer and red-shifted when compared with $[_5(CO)W(piperidine)]$ which exhibit a ligand filed transition. Ligand field and MLCT states are also emissive at low temperatures for the C_{2v} complexes. Emission in the 550 nm - 600 nm region was assigned to the lowest energy $M \rightarrow \pi^*$ excited state.[12] Emission spectra of complexes of the form $[_5(OC)W\text{-}L\text{-}W(CO)_5]$ (L = pyz, bpy, bpa) indicate two low lying emitting states, which could not be attributed to the free ligand because they are not measurably emissive following excitations.[36]

1.5.6. Objectives of the work

The objectives of this project are to synthesise some Group 6B (W and Cr) metal carbonyl complexes using N-containing heterocyclic compounds as ligands. The complexes are to be characterised using infrared, UV-visible and nuclear magnetic resonance spectroscopy, mass spectrometry, and CHN analysis. Further studies like photoluminescence and crystallography will be carried out if suitable products are obtained. The metal carbonyls to be used in this work are tungsten hexacarbonyl, $W(CO)_6$, and chromium hexacarbonyl, $Cr(CO)_6$, and the ligands are *trans*-1,2-bis(4-pyridyl)ethylene (TBE) and 3,6-di-2-pyridyl-1,2,4,5-tetrazine (DPT) (Fig. 1.5).

CHAPTER 2

2. EXPERIMENTAL

2.1. MATERIALS

The metal hexacarbonyls and the ligands were obtained from Sigma-Aldrich, UK. The solvents were bought from BDH Laboratory Supplies, England and were used without further purification; only the THF, obtained from Shalon Laboratory Supplies, was dried with molecular sieves before use. Silica gel F_{254} was obtained from Merck. The rotavapor was a BUCHI Rotavapor R-114, from BUCHI, Switzerland. The lamp for photolysis was a 125W LAM from Photochemical Reactions Ltd., U.K., and photolysis was carried out in a specially designed quartz reaction vessel fitted with a reflux condenser. Nitrogen gas used for purging was obtained from African Oxygen Ltd. (Afrox).

2.2. INSTRUMENTATION

2.2.1. Microanalysis

Microanalyses of the dinuclear *trans*-1,2-bis(4-pyridyl)ethylenetungstenpentacarbonyl and dinuclear and mononuclear 3,6-di-2-pyridyl-1,2,4,5-tetrazinechromiumpentacarbonyl dimer and monomer were carried out by the University of North London (Faculty of Science, Computing and Engineering), United Kingdom.

2.2.2. NMR Spectroscopy

^1H NMR spectra were obtained using a JNM-EX270FT NMR spectrometer, using $SiMe_4$(TMS) as the reference material. Solvents used were $CDCl_3$ for [TBE{$W(CO)_5$}$_2$] and acetone-d for [DPT{$Cr(CO_4)_2$}] and [DPT$Cr(CO)_4$].

2.2.3. Infrared spectroscopy

Infrared spectroscopy was carried out in solution cells (path length 0.5mm), using a Perkin-Elmer Paragon 1000 FTIR spectrometer (250-4000 cm^{-1}). THF was the solvent used.

2.2.4. UV-Visible spectroscopy

Electronic spectra were measured in THF on a Lambda 20 UV-Vis spectrophotometer in the range 190-1100 nm.

2.2.5. Mass Spectrometry

Mass spectra were done by the FAB (Fast Atom Bombardment) method using a Kratos MS-50 spectrometer with either 3-nitrobenzyl alcohol or CsI as a calibrant.

2.2.6. Photoluminescence spectroscopy

Luminescence spectra were taken using a Varian CARY 400 spectrophotometer. The solvent used was tetrahydrofuran (THF).

2.3. METHODS

2.3.1. Preparation of pentacarbonyl-*trans*-1,2-bis(4-pyridyl)ethylenetungsten.

0.3g (0.852 mmol) of tungsten hexacarbonyl, $W(CO)_6$, was dissolved in 200 mL dry THF, and nitrogen gas bubbled through the solution for 30 min. This solution was irradiated with an ultraviolet lamp for 5 min., and the resulting yellow solution, which contained the $[THFW(CO)_5]$ adduct, was syringed into a round bottomed flask (500 mL) containing the ligand (0.069 g, 0.38 mmol) dissolved in a minimum amount of THF under nitrogen. The reaction was left to stir overnight. The product mixture was taken to dryness with the rotavapor at 35 °C, and the dry residue contained both the mononuclear and dinuclear forms of the product. These were confirmed by TLC on silica gel plates in a hexane/THF (2:3) solvent system.

The products were separated by column chromatography using silica gel F_{254} and eluting with a hexane/dichloromethane mixture of increasing polarity. The dinuclear complex eluted first followed by the mononuclear. The dinuclear complex, which was more stable, was subjected to further analysis, but the mononuclear complex, which was unstable, could not be studied further. The

mononuclear complex decomposed to a dinuclear complex and ligand; this was confirmed by thin layer chromatographic analysis. The uncoordinated ligand nitrogen of the mononuclear complex attacks the metal to ligand nitrogen of another mononuclear complex.

CHN analysis: $[\{C_5H_4N\}_2C_2H_2\{W(CO)_5\}_2]$ Found (Calculated): %C = 31.9 (31.8); %H = 1.1 (1.2); %N = 3.2 (3.4).

2.3.2. Preparation of tetracarbonyl-3,6-(di-2-pyridyl)-1,2,4,5-tetrazinechromium

The THF method was also employed.

0.3 g (1.36 mmol) of $Cr(CO)_6$ was dissolved in 200 mL dry THF, and nitrogen gas bubbled through the solution for 30 min. This solution was irradiated with an ultraviolet lamp for 5 min., and the resulting yellow solution, which contained the $[THFCr(CO)_4]$ adduct, was syringed into a round bottomed flask (500 mL) containing 0.145 g (0.6 mmol) of the ligand, DPT, dissolved in a minimum amount of THF under nitrogen. The reaction was left to stir overnight. The product mixture was taken to dryness with the rotavapor at 35 °C, and the dry residue contained both the mononuclear and dinuclear forms of the product. This was confirmed by TLC on silica gel plates in a hexane/THF (2:3) solvent system.

The products were separated by column chromatography using silica gel and eluting with a hexane/dichloromethane mixture of increasing polarity. A green

component came out first from the column and is thought to be the dinuclear, and thereafter the blue mononuclear complex eluted. Both were quite stable and were subjected to further analysis.

CHN analysis: $[(C_5H_4N)_2C_2N_4\{Cr(CO)_4\}_2]$ Found (Calculated): %C = 47.0 (42.5); %H = 3.0 (1.4); %N = 12.0 (14.9).

CHN analysis: $[(C_5H_4N)_2C_2N_4Cr(CO)_4]$ Found (Calculated): %C = 59.0 (48.4); %H = 4.9 (2.4); %N = 13.5 (21.0)

CHAPTER 3

3. RESULTS AND DISCUSSION

3.1. *trans*-1,2-*Bis*(4-pyridyl)ethylenetungstenpentacarbonyl [TBE{$W(CO)_5$}$_2$]

3.1.1. Infra-red Spectroscopy

IR spectra of both the metal hexacarbonyl and the pentacarbonyl were run. A single band, at 1973 nm, was observed for the hexacarbonyl. The pentacarbonyl spectrum showed three bands between 1927 cm^{-1} and 1998 cm^{-1}. This is to be expected from symmetry considerations and it is also similar to results in previously published material[8]. The three bands , which are shown in Fig. 3.1, are assigned as A_1^{1b}, E and A_1^{1a} in-order of decreasing energy (cm^{-1}). The νCO stretching vibrations are listed in Table 3.1.

Table 3.1: IR stretching frequencies of [TBE$(W(CO)_5)_2$]

νCO/cm^{-1}	Intensity*	Assignment
1998	w	A_1^{1b}
1975	s	E
1927	s	A_1^{1a}

* w = Weak and s = Strong

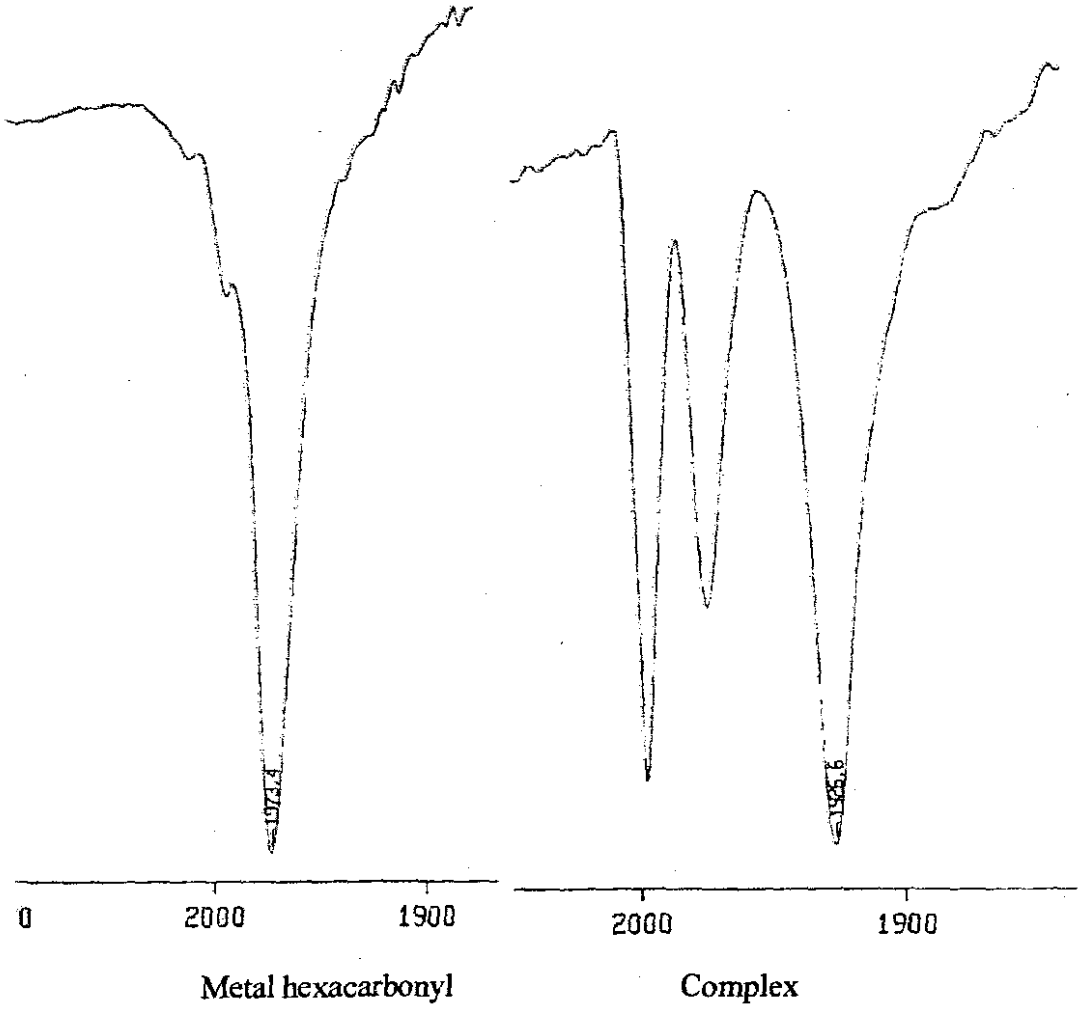

Fig. 3.1: The splitting of the CO vibration band in [TBE{$W(CO)_5$}$_2$].

3.1.2. ^{1}H NMR Spectroscopy

In this complex both the nitrogen atoms of the ligand are coordinated each to the [$M(CO)_5$] moiety. This renders the complex symmetric as the free ligand, therefore the electronic environments of the protons in the complexed ligand are essentially similar to those of the free ligand protons. The only difference now is that the electron density in the ligand has decreased upon complexation since the

lone pair of electrons on each hetero N is involved in bonding to the metal. This results in the protons of the complexed ligand being deshielded, but the structure of the spectra is expected to be the same for both ligand and complex. (Figs. 3.2 and 3.3).

The δ values for both the complex and the ligand are listed in Table 3.2. Examining the ligand signals, it can be seen that only the protons at positions 1, 3, 6, 8 are deshielded and the rest are more shielded than the protons in the complex. This is due to the fact that the deshielded protons are in close proximity to the coordinating N atoms. So the nitrogen atoms, which are more electronegative than the protons, draw the electron density away from the protons closest to them. The increased shielding of the other protons might be the result of back bonding by the metal, and these other protons must be taking the bulk of that electron density.
The fine structure of both spectra is the same i.e. two quadruplets and a doublet, the high δ values (in the region 7 to 9 ppm) confirm the aromaticity of the ring protons and the unsaturation of the ethylene protons. The doublet is due to protons 9 and 10 coupling and splitting each other's signals, which are initially singlets. The quadruplets arise from the coupling of protons 1, 3, 6, 8 and 2, 4, 5, 7 and *vice versa*. The low intensity resonances around 8.7461 and 7.0839 ppm are most probably due to impurities.

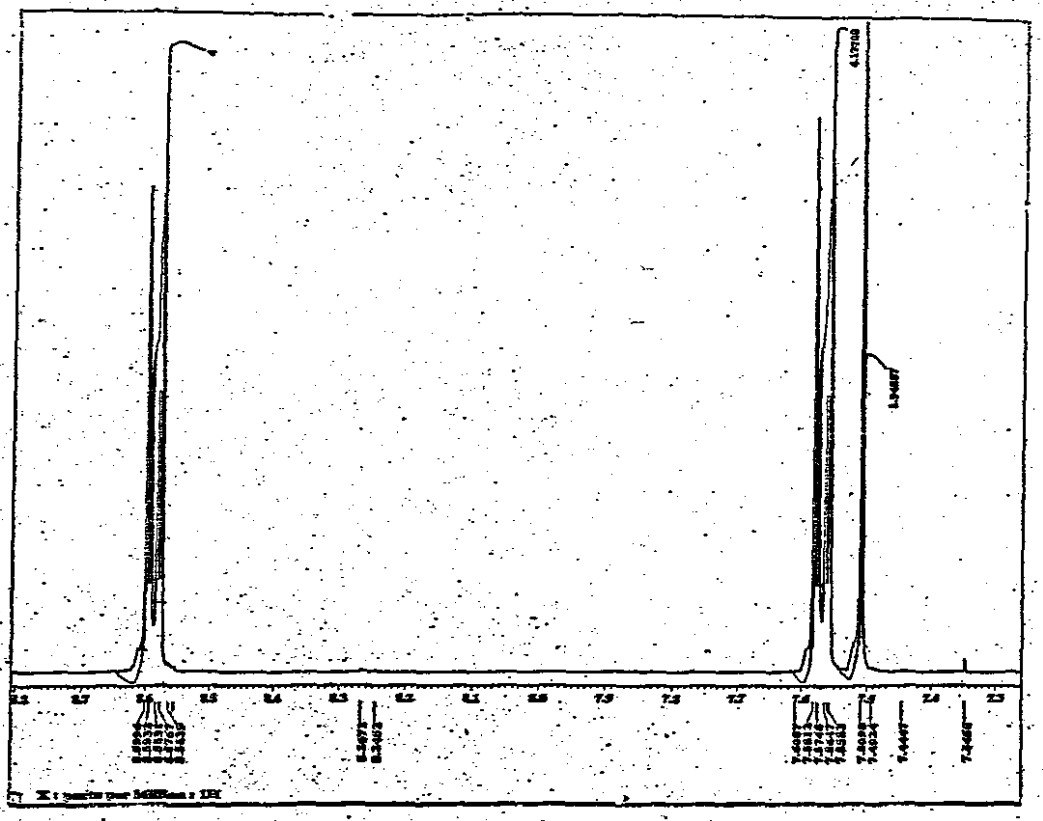

Fig. 3.2. The NMR spectrum of the ligand, TBE.

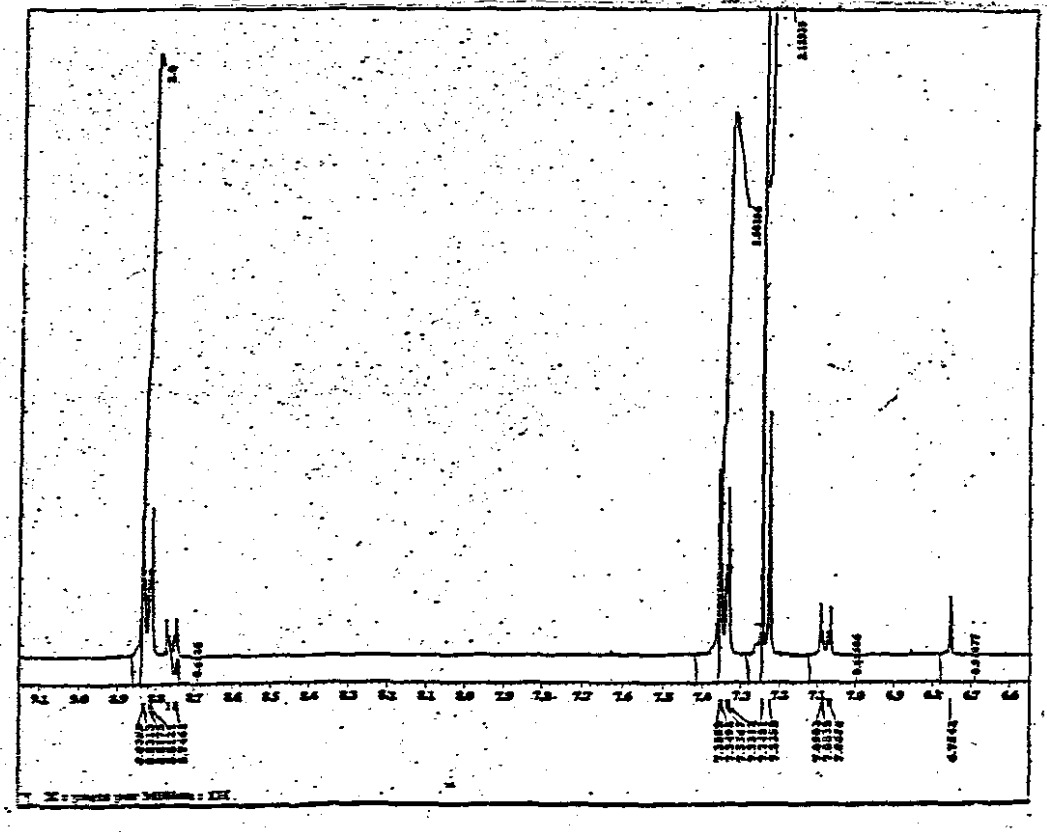

Fig. 3.3. The NMR spectrum of [TBE{$W(CO)_5$}$_2$].

The δ values are listed and assigned in Table 3.2, below.

Table 3.2: NMR signals for [TBE($W(CO)_5$)$_2$]

#H	Intensity *	Position[b]	δ	Intesity	δ(Ligand)
4	m	1, 3, 6, 8	8.82	s	8.58
4	m	2, 4, 5, 7	7.33	s	7.56
2	s	9, 10	7.24	s	7.5

* m = Medium. s = Strong, and [b]Fig. 3.4.

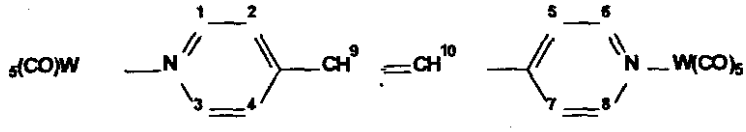

Figure 3.4. Possible structure of the complex

3.1.3. Mass spectrometry

The mass spectrum of the complex shows a distinct peak at m/e 830, which corresponds exactly with the molecular mass of the complex. Subsequent peaks show the loss of the carbonyl moiety, m/e 800, 772, 746, 719, 690, 662, 478, 450 (the last two occurring in the mononuclear species). The peak at m/e 506 corresponds to the loss of the $W(CO)_5$, since it is equal to the molecular mass of the mononuclear species.

The pyridyl cation is at m/e 79 and the complementary peak, from the ligand, is at 104. The peak at m/e 54 represents the cationic fragment $[CH_2{=}CHCH{=}CH_2]^+$, which comes from the ligand, and the one at 183 represents the ligand cation. The pattern of CO loss suggest that the mononuclear complex can lose only two carbonyls while the dinuclear can lose as many as three. The base peak at m/e 73

could not be assigned but is tentatively attributed to a ligand fragment, $[CH_3CH_2NHCH_2CH_3]^+$ arising from a rearrangement and a subsequent migration of a ligand proton. The spectrum is shown in Fig. 3.5.

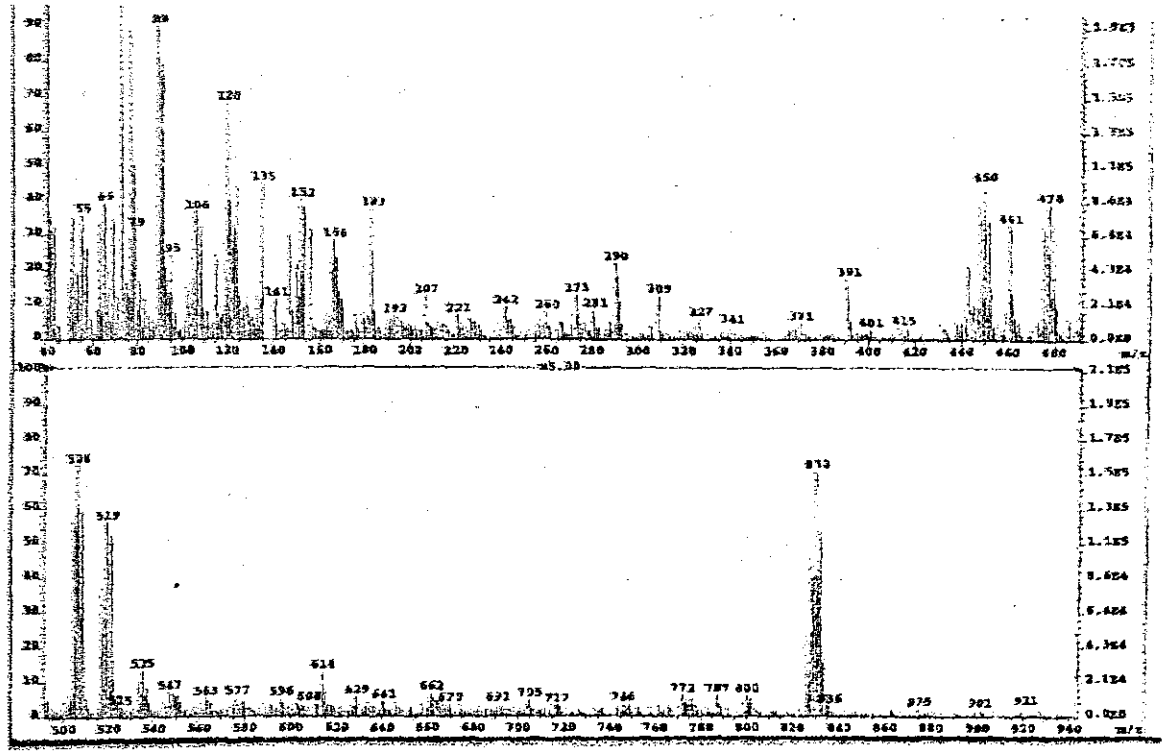

Fig. 3.5: The mass spectrum of $[TBE\{W(CO)_5\}_2]$.

3.1.4. Photoluminescence Spectroscopy

Luminescence studies were done in THF at 298 K; the excitation wavelength was 246 nm. This complex was observed to have a dual emission at 353 nm and 530 nm, with a fine structure around the second emission[36]. The low energy emission

(530 nm) is thought to be of MLCT in character because of the its lower energy position, resulting from the π^* orbital stabilisation (LUMO) by the metal centres in the complex. The other emission is of ligand character since it occurs at high energy. The spectrum is shown in the Fig 3.6.

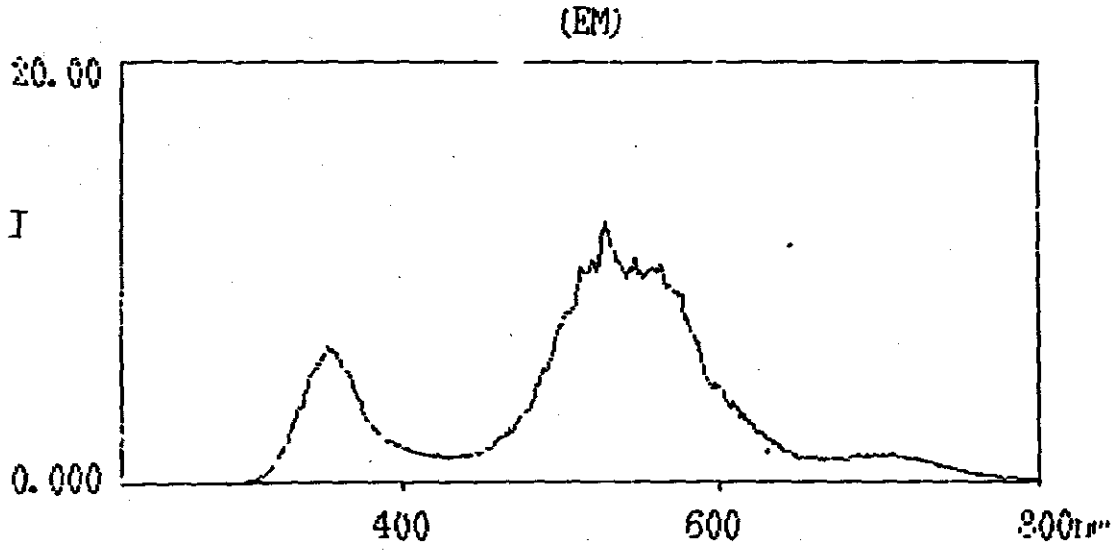

Fig. 3.6. Emission spectrum of [TBE{$W(CO)_5$}$_2$].

3.2. 3,6-Di-2-pyridyl-1,2,4,5-tetrazinechromiumtetracarbonyl.

3.2.1. Infrared spectroscopy

Since the ligand has two pairs of nitrogen atoms in close proximity, it is assumed that both pairs of the lone pair electrons will attack the chromium hexacarbonyl. This will produce a *cis*-[LCr(CO)$_4$] complex where L is the ligand, and the *cis*-dinuclear complex will be [$_4$(CO)CrLCr(CO)$_4$] since the ligand still has two unbonded nitrogen atoms in close proximity (Fig. 3.7.).

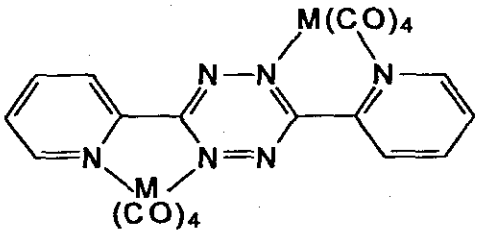

Dimeric DPT complex

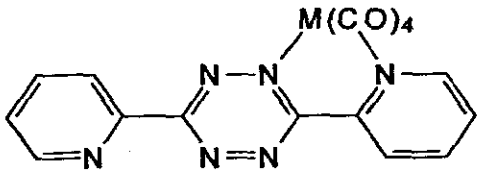

Monomeric DPT complex

Fig. 3.7. Possible structure of the chromium complexes with DPT

As explained in chapter 1, here we expect four IR active bands,

viz. A_1^{1a}, B_1, A_1^{1b}, and B_2. The actual IR frequencies are listed in Tables 3.3 and 3.4.

Table 3.3: IR stretching frequencies for $[DPT(Cr(CO)_4)_2]$

$\nu CO/cm^{-1}$	Intensity	Assignment
2028	vw	A_1^{1a}
1976	s	B_1
1923	s	B_2
1872	m	A_1^{1b}

Table 3.4: IR stretching frequencies for $[DPTCr(CO)_4]$

$\nu CO/cm^{-1}$	Intensity	Assignment
2012	s	B_1
1930	vs	B_2
1878	s	A_1^{1b}

vs = Very strong; s = Strong; vw = Very weak

The A_1^{1a} band, which is the weakest, is not resolved in this spectrum; this may be due to the solvent effects and to the fact that only one $[Cr(CO)_4]$ moiety is absorbing the radiation. The band at 1923 cm^{-1} in the dinuclear complex appears broadened and weaker than the corresponding band at 1930 cm^{-1} in the mononuclear complex. The spectra are shown in Figs. 3.8. and 3.9 .

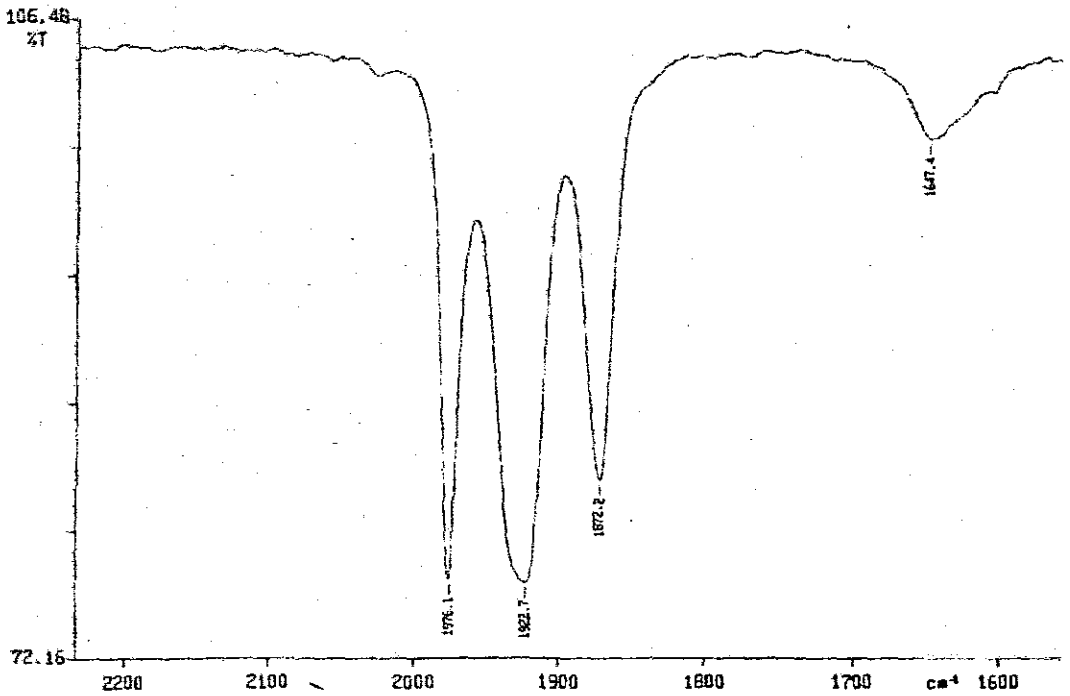

Fig. 3.8. IR splitting of the CO vibration band in [DPT{$Cr(CO)_4$}$_2$]

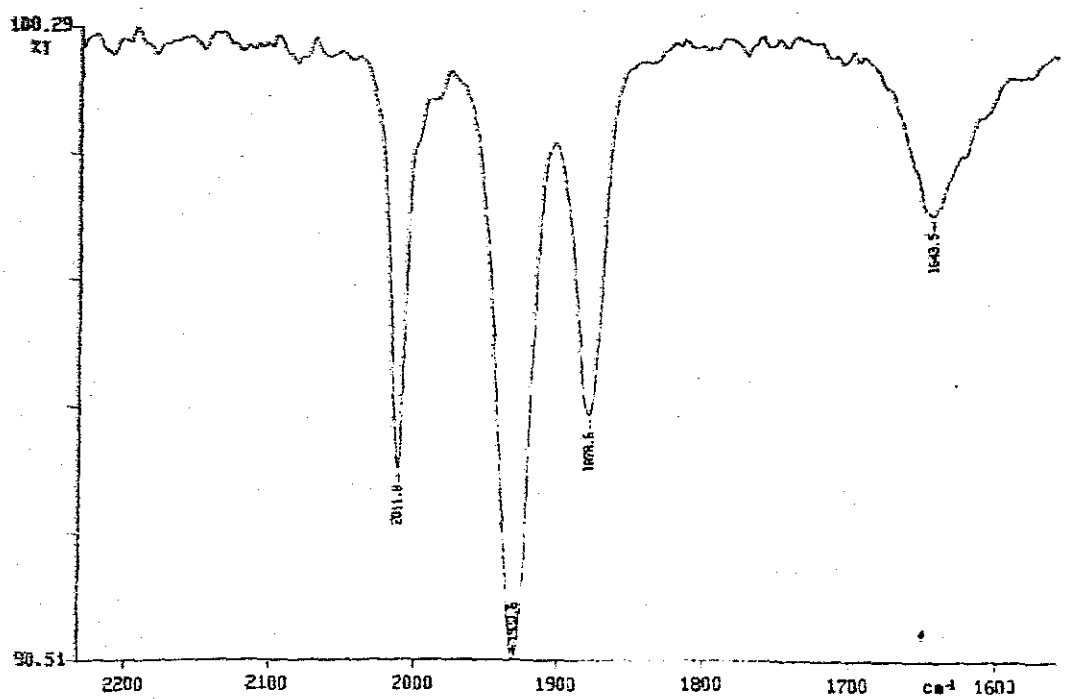

Fig. 3.9. IR splitting of the CO vibration band in [DPTCr$(CO)_4$]

3.2.2. NMR spectroscopy

The spectra of the free ligand, the dinuclear and the mononuclear complexes were run. As expected, the spectra of the dinuclear and free ligand were similar, with that of the dinuclear deshielded. The similarity between the ligand and the dinuclear complex spectra is because the symmetry of the ligand in the dinuclear complex is unaltered by coordination since coordination sites are similar (Fig. 3.7.). The symmetry is therefore similar. The observed deshielding results from electron donation by the ligand to the metals through its nitrogen atoms, so the electron density on the N atoms is less in the complex. The spectrum of the mononuclear is radically different from that of the dinuclear and that of the free ligand, indicating a loss of symmetry since only one side of the ligand is coordinated. The δ values are shown in Table 3.5, and the spectra in Figs. 3.10, 3.11 and 3.12. As can be seen from Figs. 3.10 and 3.12, only four signals were observed for both the dinuclear complex and the ligand; each signal is due to two protons. Protons close to the nitrogen atom (i.e. 1, 8) resonate at high field compared to those that are two or three bonds away from the highly electronegative nitrogen atoms. Signals for protons 1, 8 and 4, 5 are quadruplets, this is because each of the two protons is coupled to another e.g. for protons 1 and 8, 1 is coupled to 2 and 8 to 7. The same applies for protons 4 and 5, 4 coupled to 3 and 5 to 6. Signals for 2, 7 and 3, 6 are octuplets since each proton is coupled to two other protons, e.g. 2 is coupled to 1 and 3, and 7 is coupled to 6 and 8; same

for 3 and 6, 3 couples to 2 and 4, and 6 to 5 and 7. So the initial doublet is split twice to make the octuplet.

From the spectrum of the mononuclear complex and the δ values in Table 3.5, it can be seen that each proton resonates individually and they are also deshielded. This is due to the loss of symmetry in the ligand that accompanies the coordination of the metal centre to close-neighbour pair of N atoms located on one side of the ligand. The aromaticity and unsaturation is reflected in the high δ values of the spectra (7 to 9 ppm).

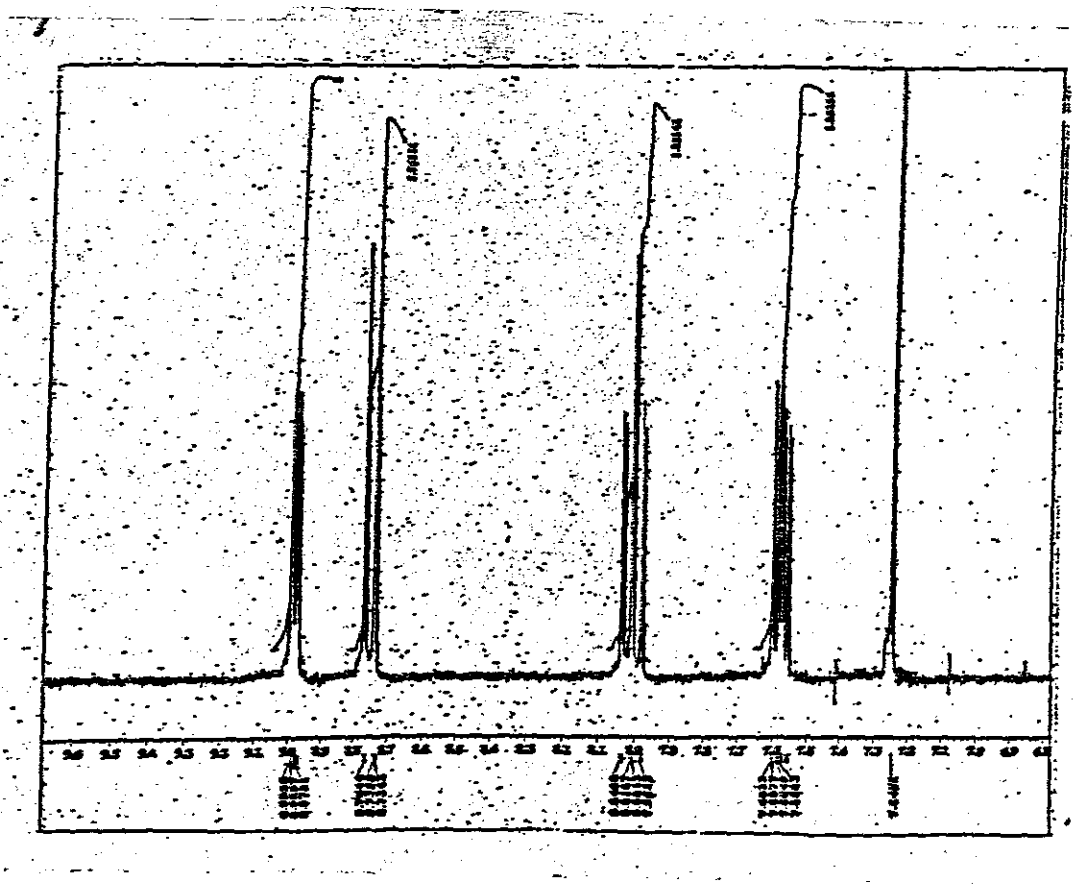

Fig. 3.10 The NMR spectrum for the ligand, DPT.

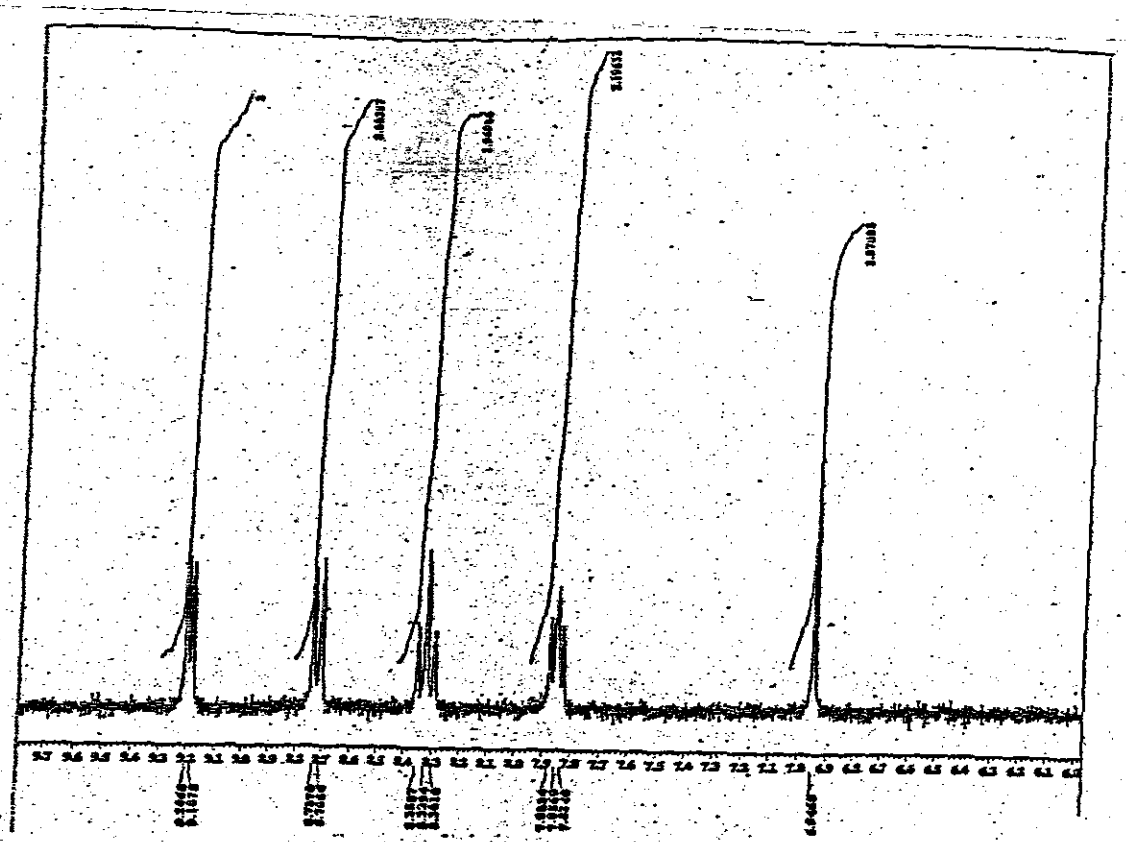

Fig. 3.11 The NMR spectrum for the complex, [DPT{$Cr(CO)_4$}$_2$]

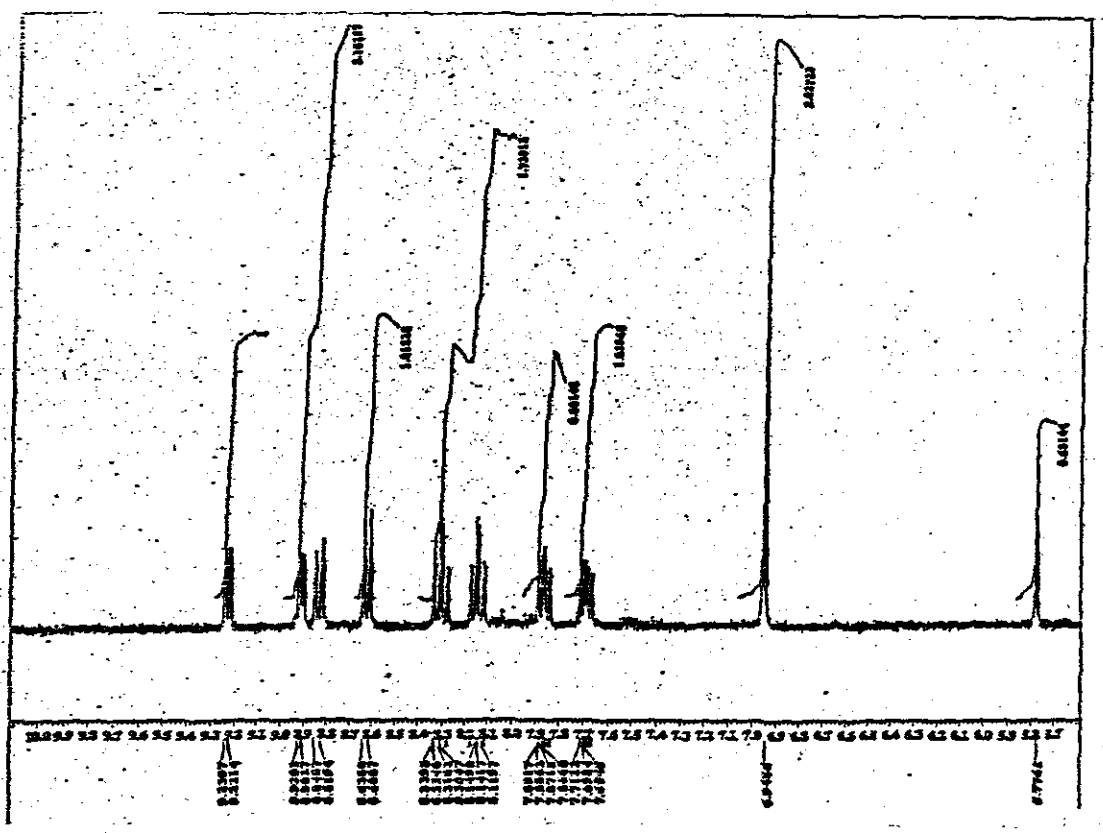

Fig. 3.12. The NMR spectrum for the complex, [DPT$Cr(CO)_4$]

Table 3.5: ^{1}H NMR δ value for [DPT{Cr(CO)$_4$}$_2$].

Complex	Signals			
	# H atoms	Intensity	Positions*	δ
[DPT{Cr(CO)$_4$}$_2$]	2	m	1, 8	9.2
	2	m	4, 5	8.7
	2	m	2, 7	8.3
	2	m	3, 6	7.8
[DPTCr(CO)$_4$]	1	m	1	9.2
	1	m	2	8.9
	1	m	4	8.8
	1	m	3	8.6
	1	m	8	8.3
	1	m	7	8.1
	1	m	5	7.8
	1	m	6	7.6
DPT	2	m	1, 8	8.98
	2	m	4, 5	8.75
	2	m	2, 7	8.01
	2	m	3, 6	7.58

*Fig. 3.13.

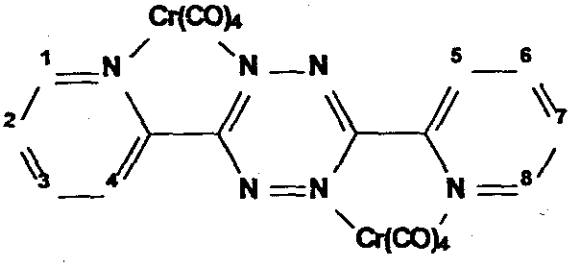

Figure 3.13. Carbon positions for the resonating protons.

3.2.3. UV-Visible spectroscopy

The spectra of both the dinuclear and the mononuclear complexes show the expected transitions, i.e. intraligand, MLCT, and ligand field transitions. As shown in Table 3.6 the first three transitions, between 279 nm and 383 nm, are similar in both spectra. This suggests that they are intraligand in character. The high energies of these transitions support the assignment. The mononuclear MLCT assignment is at 653 nm, but the dinuclear one, which also has high intensity, is at 901 nm. This is due to the lowering of the π^* orbital energy of the ligand upon dimerisation. The d-d/ LF transition occurs at 909 nm and at 1050 nm for the mononuclear and their low intensities due to them being not allowed. The high intensity of the MLCT transition of the dinuclear complex is further evidence of the lowering of the π^* orbital of the ligand, increasing the ease of the transition.. The band positions are listed and assigned in Table 3.6. The spectra are shown in Figs. 3.14 and 3.15.

Table 3.6: UV-Vis values for DPT based complexes.

$DPTCr(CO)_4$		$DPT(Cr(CO)_4)_2$	
λ/nm	Transition	λ/nm	Transition
279.97	IL	279.97	IL
303.53	IL	303.53	IL
382.75	IL	382.75	IL
652.52	MLCT	900.88	MLCT
909.45	LF		

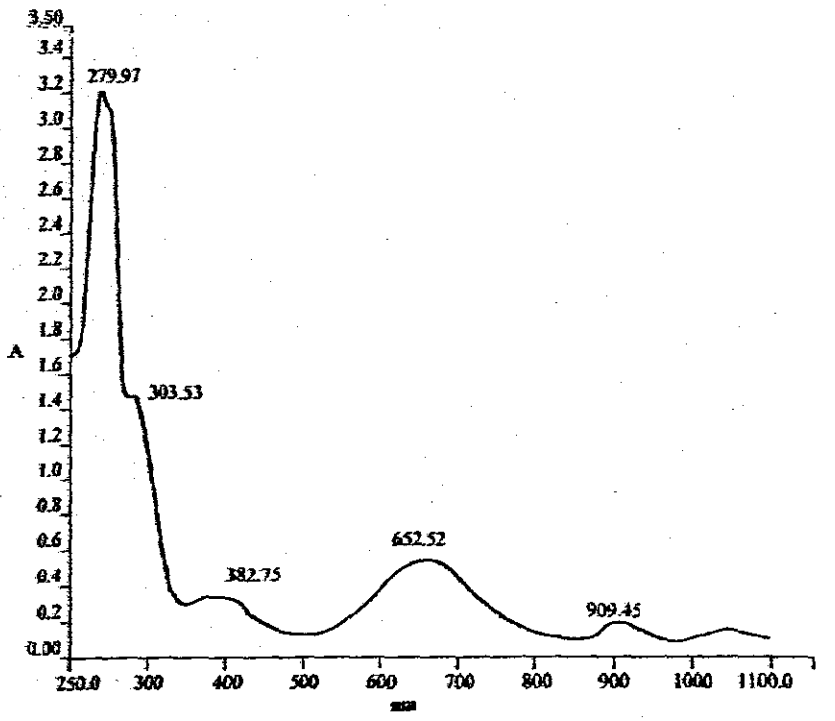

Fig. 3.14. UV-visible spectrum for the complex, [DPTCr(CO)$_4$]

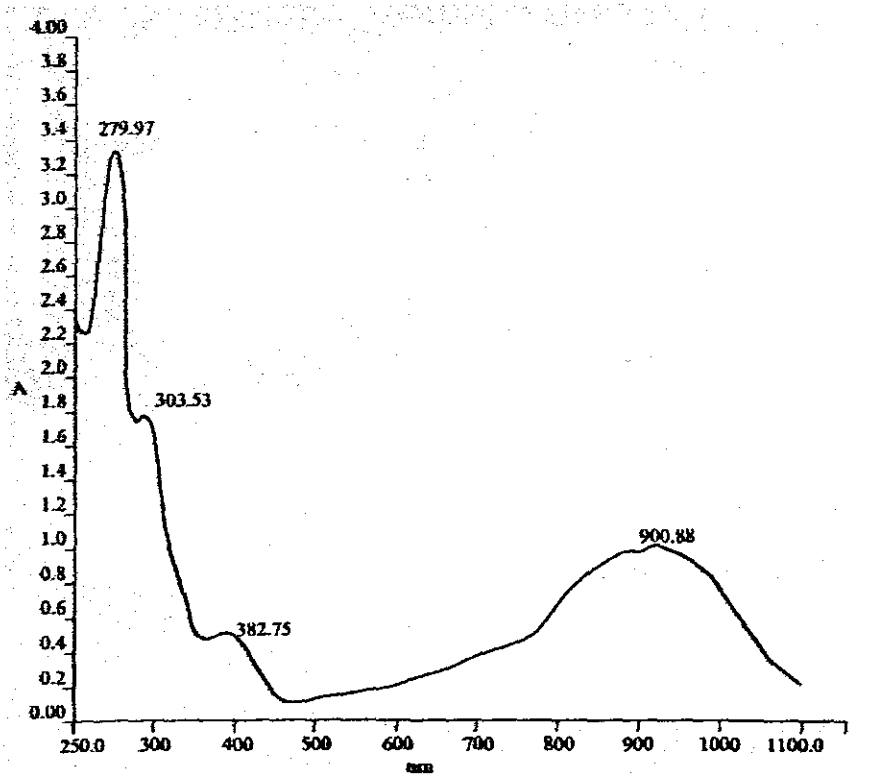

Fig. 3.15. UV-Visible spectrum for the complex, [DPT(Cr(CO)$_4$)$_2$]

3.2.4. Photoluminescence

Both the mononuclear and dinuclear complexes were subjected to luminiscence studies, using THF as a solvent at 298 K. An excitation wavelength of 250 nm was applied and both complexes gave single, broad emissions, at 460 nm for the mononuclear and at 523 nm for the dinuclear. The lower energy emission in the dinuclear complex occurs because of the stabilisation of the π^* orbital of the ligand by the two metal centres in the complex, thus making the energy of separation between the HOMO (metal d orbital) and the LUMO (π^* orbital of the ligand) smaller[14]. For the mononuclear complex the stabilisation is smaller than in the dinuclear complex since only one metal centre is attached to the ligand. The spectra are shown in Figs. 3.16 and 3.17 for the mononuclear and dinuclear complexes respectively. There is a shoulder in the spectrum for the dinuclear complex (Fig. 3.17). This is due to the fine structure of the emission spectrum. The fine structure of a spectrum is a product of the rearrangement the molecule undergoes on its path from the excited state arrangement to a deactivated state accompanied by loss of absorbed energy. In the same figure, a small peak around 400 nm is observed and this is tentatively attributed to ligand emission because of its higher energy compared to the main peak.

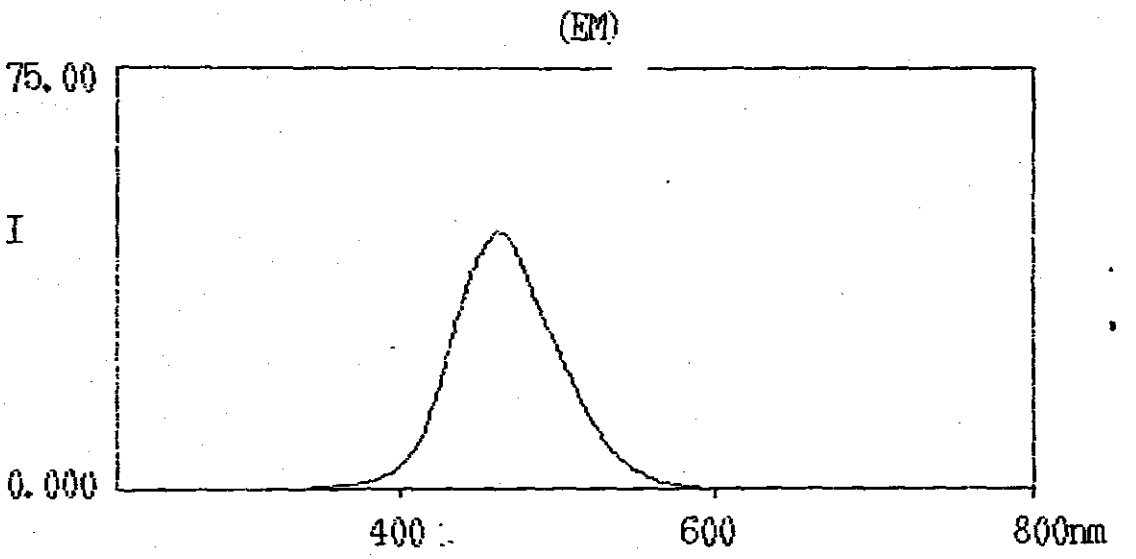

Fig. 3.16. Emission spectrum of [$Cr(CO)_4$-DPT]

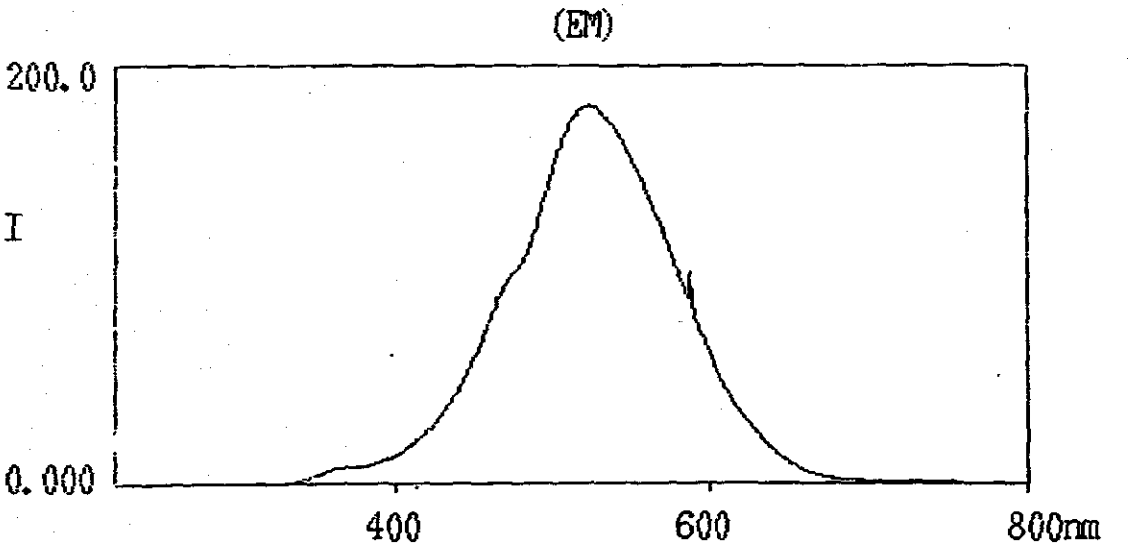

Fig. 3.17. Emission spectrum of [$\{Cr(CO)_4\}_2$-DPT]

CHAPTER 4

CONCLUSION

The main problem encountered in this work is the lack of stability of some of these complexes; some metal/ligand combinations did not work. In the case of tungsten hexacarbonyl and 1,2-bis(4-pyridyl)ethylene (TBE), the dinuclear complex was very stable whilst its mononuclear analogue was not. This could be attributed to the reactivity of the uncoordinated nitrogen atom of the ligand of the mononuclear complex, which attacks the metal centre of the second mononuclear moiety, generating a free ligand and the dinuclear complex. This thinking is supported by TLC analysis; where the initial analysis gave one spot, but the TLC analysis after some time gave three spots corresponding to the dinuclear, mononuclear and the ligand. Working at low temperatures and in a dark environment might ameliorate this problem by lowering the kinetic energy of the complexes, and reduce photochemical interactions between them.

Another case in point is that of the complexes formed from $W(CO)_6$ and 3,6-(di-2-pyridyl)-1,2,4,5-tetrazine (DPT), and $Cr(CO)_6$ and DPT. The former complexes were extremely unstable and the latter were very stable, under similar conditions. The reason for this could only be the different atomic sizes of the metals, since the ligand is the same.

The stable complexes were further characterised using infrared, NMR, mass spectrometry and microanalysis. The CHN analysis for $[DPT\{Cr(CO)_4\}_2]$ and

[DPTCr(CO)$_4$] appeared bad even though the TLC of the complexes gave one spot each.

The presence of the MLCT transition was observed using UV-Vis electronic spectroscopy. The position of this transition was sensitive to the number of metal centres in the complex. It was considerably red shifted in the dinuclear complex as compared to the mononuclear. The complexes were also found to be luminescent, with the dinuclear complexes giving a single broad MLCT emission whilst the mononuclear gave two emissions, one due to the ligand and the other due to MLCT transitions.

Future studies should concentrate on the electrochemical and photochemical properties of these complexes. The electrochemistry should be investigated to ascertain the redox behaviour of the complexes and therefore establish if they are potentially useful in solar energy harvesting technology. Mixed metal complexes should also be included in further investigation. Techniques like cyclic voltammetry and electron spin resonance spectroscopy could be of use in achieving these objectives. Photochemical stability is important if these complexes are to be used in light energy harvesting technology. The electronic structure of the complexes, which varies according to the metal centre and the ligand, affects the nature of the photochemical reactions they could undergo. In some instances, the carbonyl is preferentially lost whilst in others it is the ligand that is lost.

REFERENCES

1. Furholz, U., Burgi, H-B, Wagner, F.E., Stebler, A., Ammeter, J.H., Krausz, E., Clark, R.J.W., Stead, M.J. and Ludi, A., *J. Am. Chem. Soc.*,1984, 106, 121-123.
2. Creutz, C. and Taube, H.J., *J. Am. Chem. Soc.*, 1969. 91, 3988-3991.
3. Jaradat, Q., Barquis, K., and Akasheh, T.S., *Inorganic Chimica Acta*, 1986, 116, 63-73.
4. Kaim, W., and Kohlmann, S., *Inorg. Chem.*, 1990, 29, 2909-2914.
5. Kaim, W., Ernst, S. and Kohlmann, S., *Polyhedron*, 1986,Vol. 5, No. 12, 445-449.
6. Haim, A., Chem. Res., 1975, 8, 264-267
7. Ruminski, R. and Peterson, J.D., *Inorg. Chem.*, 1982, 21, 3706-3709.
8. Norton, K.A., and Hurst, J.K., *J. Am. Chem. Soc.*, 1982, 104, 5960-5964.
9. Curtis, J.C., Bernstein, J.S., and Meyer, T.J., Inorg. Chem., 1985, 24, 385-387.
10. Kohlmann, S., Ernst, S. and Kaim, W., *Angew. Chem. Int. Ed. Engl.*, 1985, 24, No. 8, 684-685.
11. Campagna, S., Denti, G., De Rosa, G., Sabatino, L., Ciano, M. and Balzani, V., *Inorg. Chem.*, 1989, 28, 2565-2570.
12. Lees, A.J., Fobare, J.M. and Mattimore, E.F., *Inorg. Chem.*, 1984, 23, 2709-2713.
13. Zulu, M.M. and Lees, A.J., *Inorg. Chem.*, 1988, 27, 1139-1145.
14. Kolodziej, R.M. and Lees, A.J., *Organometallics*, 1986, 5, 450-455.

15. Manuta, D.M. and Lees, A.J., Inorg. Chem., 1986, 25, 1354-1359.

16. Kim, Y. and Lieber, C.M., *Inorg. Chem.*, 1989, 28, 3990-3992.

17. Powers, M.J. and Meyer, T.J., *J. Am. Chem. Soc.*, 1980, 102:4, 1289-1297.

18. Peterson, J.D., Murphy, W.R. Jr., Sahan, R., Brewer, K.J. and Ruminski, R.R., *Coord. Chem. Rev.*, 1985, 64, 261-272.

19. Geoffroy, G.L. and Wrighton, M.S., 1979, 1st Ed., 2-4

20. Sanshiro Komiya, Synthesis of Organometallic Compounds, 1st Ed., 1997.

21. Wrighton, M.S., Hammond, G.S. and Gray H.B., *J. Am. Chem. Soc.*, 1971, 93, 4336-4339.

22. Wrighton, M.S., Abrahamson, H.B. and Morse, D.L., *J. Am. Chem. Soc.*, 1976, 98, 4105-4109.

23. Wrighton, M.S.and Abrahamson, H.B., *Inorg. Chem.*, 1978, 17, 3385-3391.

24. Dahlgren, R.M., and Zinc, J.L., *Inorg. Chem.*, 1977, 16, 3154-3157.

25. Schwenger, G., Darensbourg, M.Y., and Darensbourg, D.J., *Inorg. Chem.*, 1972, 11, 1967-1971.

26. Darensbourg, D.J., and Murphy, M.A., *Inorg. Chem.*, 1979, 17, 884-886.

27. Gaus, P.L., Boncella, J.M., Rosengren, K.S., and Funk, M.O., *Inorg. Chem.*, 1982, 21, 2174-2177.

28. Elschenbroich, Ch. and Salzer, A., Organometallics, 1st Ed., 1989.

29. Kranenburg, M.J., *J. Am. Chem. Soc.*, Chem. Commun., 1995, 2177-2179.

30. Gilchrist, T.L., Heterocyclic Chemistry, 1085, 1st Ed., pp5.

31. Staal, L. H., Stufkens, D.J., Oskam, A., *Inorg. Chim. Acta.*, 1978, 26, 255-259.

32. Das, A., Maher, J.P., Mclleferty, J.A., Badiola, N.J.A., and Ward, M.D., *Chem. Soc.*, Dalton Trans.,1993, 681-686.

33. Zulu, M.M., and Lees, A.J., *Organometallics*, Vol. 8, No. 4, 1989, 955-960.

34. Brewer, K.J., Murphy, W.R.,Jr., and Pieterson, J.D., *Inorg. Chem.*,26, 1987, 3376-3379.

35. Kaim, W. and Kohlmann, S., *Inorg. Chem.*, 26, 1987, 68-77.

36. Nel, A., Chapman, J., Long, N.J., Kolawole, G. A., Motevalli, M., O'Brien, P., *Polyhedron*, 19 (2000) 1621-1626.

APPENDIX A: Structure of the Pentacarbonyltrans-1,2-(bis-4-pyridyl)ethylenetungsten[36].